

## The surface of constant rate of energy dissipation under creep and its experimental determination

Z. KOWALEWSKI (WARSZAWA)

THIS PAPER presents the results of creep experiments in which thin-walled tubular test pieces of M1E pure copper (according to Polish Standards) were loaded by combined tension and torsion in elastic region at 573K. The theory of creep potential is used to determine the theoretical surface of constant rate of energy dissipation. The paper describes the construction of high temperature bi-axial creep machine and mechanical extensometer which transmits the deformation of the specimen gauge length outside the furnace. The method of determining the surface of constant rate of energy dissipation on the basis of experimental results is discussed.

W pracy przedstawiono wyniki prób pełzania dla czystej miedzi elektrolitycznej M1E w temperaturze 573 K. Badania prowadzono w płaskim stanie naprężenia realizowanym na cienkościennych próbkach rurkowych przez różne kombinacje siły osiowej i momentu skręcającego w obszarze sprężystym. Dla zilustrowania techniki pomiarowej zamieszczono opis budowy stosowanej pełzarki oraz ekstensometru mechanicznego, umożliwiającego transmisję odkształcenia części pomiarowej próbki na zewnątrz pieca. Bazując na teorii potencjału pełzania, określono teoretyczną powierzchnię stałej prędkości dysypacji energii. Materiał doświadczalny z przeprowadzonych badań posłużył do opracowania metodyki wyznaczania rzeczywistego kształtu powierzchni pełzania.

В работе представлены результаты испытаний ползучести для чистой электролитической меди М1Е в температуре 573 К. Исследования проводились в плоском напряженном состоянии, реализованном на тонкостенных трубчатых образцах путем разных комбинаций осевой силы и скручивающего момента в упругой области. Для иллюстрации измерительной техники помещено описание строения применяемой крип-установки и механического экстензогра, который дает возможность передачи деформации измерительной части образца наружу печи. Базируя на теорию потенциала ползучести, определена теоретическая поверхность постоянной скорости диссипации энергии. Экспериментальный материал, из проведенных исследований, послужил для разработки методики определения действительной формы поверхности ползучести.

### 1. Introduction

THE VAST majority of experimental creep results presented in the literature were obtained under uni-axial states. The actual development of technology necessitates further investigation of creep phenomena under multiaxial stress conditions. Creep design for machine parts (for example in steam turbines, reactors) subject to high multiaxial states of stress and working at high temperature requires such experiments.

Most creep theories are based on the assumption that the material is isotropic which simplifies the considerations. Possibility of determination of material constants in uni-axial tests and formulation of the theory for complex states is an advantage of such an

approach. In the case of potential theory it leads to the assumption of the creep potential in the form of the second invariant of the stress tensor. Such potential has a geometrical representation in the form of an ellipsoid in the stress space.

Recently, in view of an increasing number of creep investigations under complex stress states, a tendency to analyse the creep data under the assumption of existence of the creep surface is observed [1, 2, 3].

In the paper is proposed a programme of model testing under plane state of stress which makes it possible to determine the surface of constant rate of energy dissipation.

## 2. Creep potential theory

Theory of plastic flow of materials is based on the assumption that the plastic potential exists. In practice, for isotropic material, the plastic potential function is usually identified with the condition  $F(J_1, J_2, J_3) = 0$  which expresses the yield condition, where  $J_1, J_2, J_3$  denote the stress tensor invariants. In such a case the strain rate tensor  $\dot{\epsilon}_{ij}$  is connected with stresses by relation

$$(1) \quad \dot{\epsilon}_{ij} = \lambda \frac{\partial F(J_1, J_2, J_3)}{\partial \sigma_{ij}},$$

which is called the flow rule associated with the yield condition.

The concept of plastic potential has been transferred to the creep theory in analogous form. For both the first and second stages of creep the existence of the creep potential  $\Phi$  is assumed which depends on time and on the parameters describing the state of material. Then the creep rate is determined by the expression

$$(2) \quad D_{ij} = \frac{\partial \Phi}{\partial \sigma_{ij}}.$$

In the case of steady state of creep, the rate is expressed in the form of generalized Norton's equation

$$(3) \quad D_{ij} = k \sigma_{ij}^n,$$

where  $k, n$  are material constants which depend on temperature and are determined from uni-axial tests.

Equation (3) can be presented, for a given material, in a more convenient, dimensionless form

$$(4) \quad \frac{D_{ij}}{D_0} = \left( \frac{\sigma_{ij}}{\sigma_0} \right)^n.$$

In paper [4] generalized forms of Eqs. (3) and (4) were applied,

$$(5) \quad D_{ij} = \frac{\partial \psi}{\partial \sigma_{ij}}, \quad \psi = \frac{D_0 \sigma_0}{n+1} \Phi^{n+1},$$

where  $\Phi$  is a homogeneous, dimensionless function differentiable in the stress space  $\sigma_{ij}/\sigma_0$ ; it assumes the value of unity in the case of uni-axial tension at the stress level  $\sigma_0$ . The full, dimensionless form of the equation is expressed by the relations

$$(6) \quad \frac{D_{ij}}{D_0} = \Phi^n \frac{\partial \Phi}{\partial (\sigma_{ij}/\sigma_0)}$$

and

$$(7) \quad \frac{L}{L_0} = \frac{\sigma_{ij} D_{ij}}{\sigma_0 D_0} = \Phi^{n+1},$$

where  $L$  is the rate of energy dissipation.

Surfaces of constant values of function  $\Phi$  in the stress space express the constant rate of energy dissipation. These surfaces are convex, similar and coaxial and, in the case of isotropic body under steady creep conditions, they are defined by the relation

$$(8) \quad \Phi = \frac{\sigma_i}{\sigma_0} = \text{const.}$$

Taking into account Eq. (8), relation (6) yields

$$(9) \quad \frac{D_{ij}}{D_0} = \frac{3}{2} \left( \frac{\sigma_i}{\sigma_0} \right)^{n-1} \frac{s_{ij}}{\sigma_0}.$$

Final form of this equation is analogous with Odqvist's equation for complex stress state under the assumption that the material is isotropic and incompressible, and that hydro-tatic pressure has no influence on the creep rate. The creep potential in the case of isotropic hardening can then be expressed as a function of the second and third invariants of the stress deviator  $S_{ij}$ . In the case of plane state of stress the creep potential may be expressed by the function

$$(10) \quad \Phi = [(\sigma_{11}^2 - \sigma_{11}\sigma_{22} + \sigma_{22}^2 + 3\sigma_{12}^2)/\sigma_0^2]^{1/2} = \text{const.}$$

Equation (10) corresponds to the ellipsoid in the stress space (Fig. 1) as in the theory of plasticity [5]. Some characteristic ellipses which correspond to different loading paths of a specimen can be distinguished on the surface of the ellipsoid. The ellipse passing

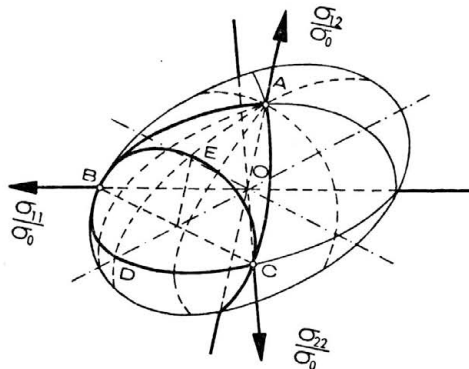


FIG. 1. Surface of a constant rate of energy dissipation based on the Huber–Mises condition for plane state of stress.

through points  $A, B$  corresponds to the case of a combination of an axial force and a torque. Ellipse  $AC$  represents such states of loading which are obtained by a torque and pressure. The ellipse passing through points  $B, D, C$  corresponds to simultaneous loading of tubular specimens by an axial force and a pressure. In the case of plane specimens it is possible to obtain such states of stresses which correspond to uni-axial tension in different directions with respect to the axis  $\sigma_{11}/\sigma_0$  and are represented by the ellipse  $BEC$ .

The ellipsoid presented in Fig. 1 is a theoretical surface of constant rate of energy dissipation under creep, determined by assuming the potential function in the form of the second invariant of the stress deviator.

Assumption of the existence of a potential makes it possible to formulate the creep theories for materials with hardening by introducing to the function one or several parameters which depend on the creep deformation, temperature and time. In paper [7] was discussed the constitutive model of creep based on the concept of kinematic hardening in which creep potential for plane state of stresses, induced by a combined action of tension and torsion, is expressed by formula

$$(11) \quad \Phi = \frac{\mu}{n+1} \{[(\sigma_{11} - \alpha_{11})^2 + 3(\sigma_{12} - \alpha_{12})^2]^{1/2}\}^{n+1},$$

where  $\alpha_{11}, \alpha_{12}$ —parameters defining the position of creep surface.

This model was used for description of creep under cyclic loading. The form of the creep potential corresponds to the ellipsoid in the stress space. Similar form of the potential was also assumed in [6] and [8], where the creep potential theory was used to describe the influence of the direction and value of the initial plastic deformation on the steady creep rate of plane and tubular specimens.

### 3. Description of specimens and testing machine

The thin-walled tubular specimens with dimension shown in Fig. 2 were used in the test. Specimens were machined from a drawn rod made of commercially pure electrolytic copper denoted by M1E (according to Polish Standards). The material was cut out and then annealed at 673 K for two hours and furnace cooled. The aim of the thermal treatment was to obtain a homogeneous structure of the material tested. Experiments were performed on the creep device shown in Fig. 3. The device makes it possible to investigate the creep phenomena in thin-walled tubular specimens loaded by a combination of tension and torsion at elevated temperatures. The complex state of stress was introduced by two independent loading systems applying torsion and tension. The tension system is of dead weight-lever type while the torsion system is of dead weight-pulley type. A portion of the kinematic chain of the loading system is shown in Fig. 4. Specimen (1) (Fig. 3) is pinned to two vertical rods, the lower one (3) is connected with a threaded mandrel used for horizontal adjustment of the position of the lever, while the upper rod (2) is connected, through a load cell (6) and an air bearing (7), with the horizontal lever (9). An air bearing is used to enable the loading systems to work independently. The device enables us to produce an air cushion which ensures transmission of the axial load and elimi-

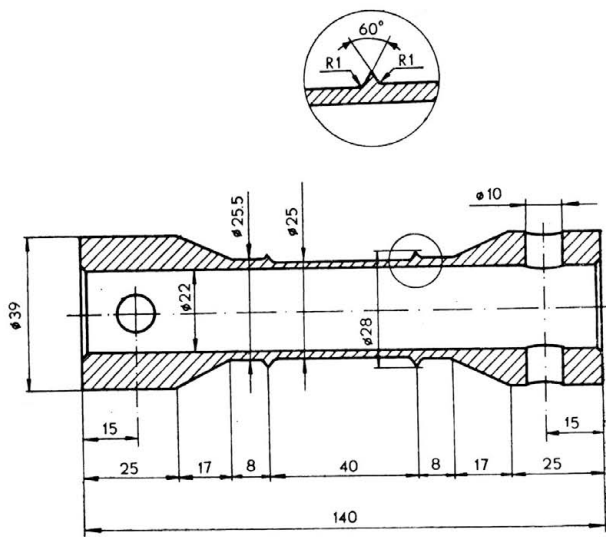


FIG. 2. Specimen.

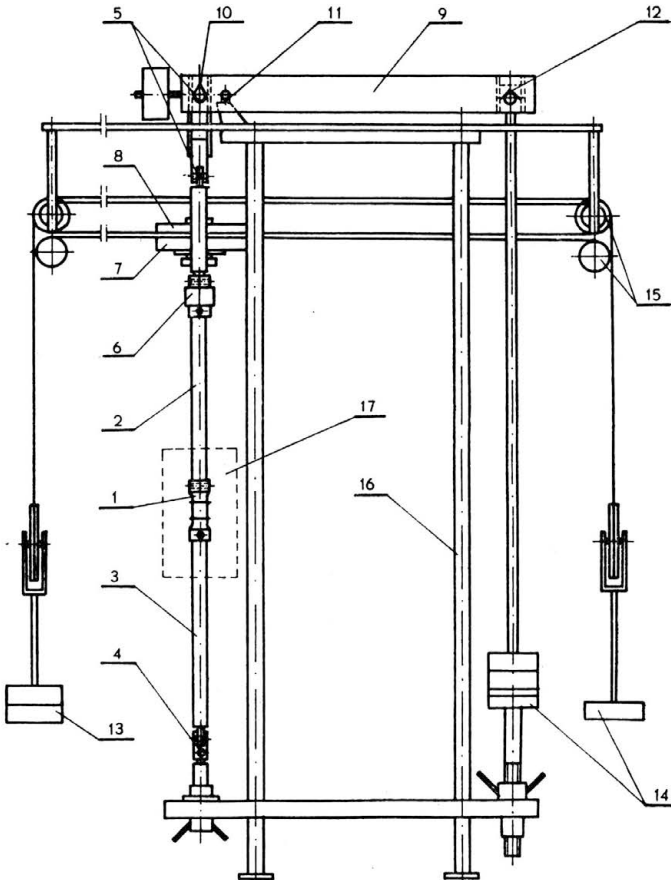


FIG. 3. Creep machine: 1—specimen, 2—upper rod of loading system, 3—lower rod of loading system, 4, 5—universal joints, 6—load cell, 7—air bearing, 8—torque disc, 9—horizontal lever, 10, 11, 12—knife edges, 13, 14—dead weights, 15—pulleys, 16—frame, 17—furnace.

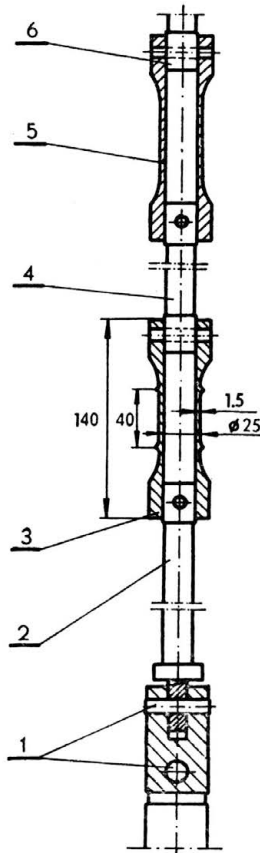


FIG. 4. Mounting of specimen: 1—universal joint, 2—lower loading rod, 3—specimen, 4—upper loading rod, 5—load cell, 6—torque disc shaft.

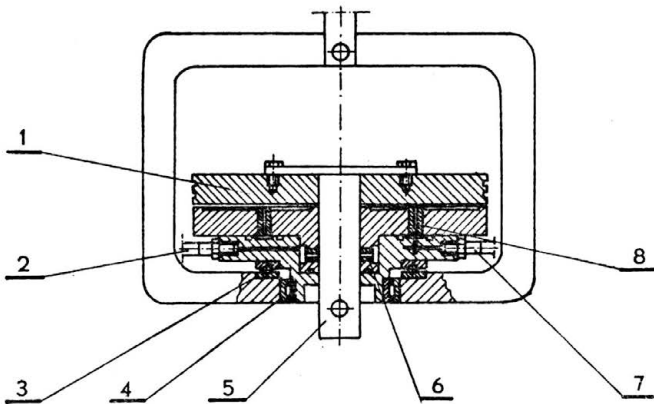


FIG. 5. Air bearing: 1—torque disc, 2, 7—air inlets, 3—ball bearing, 4—roller bearing, 5—torque disc shaft, 6, 8—air nozzles.

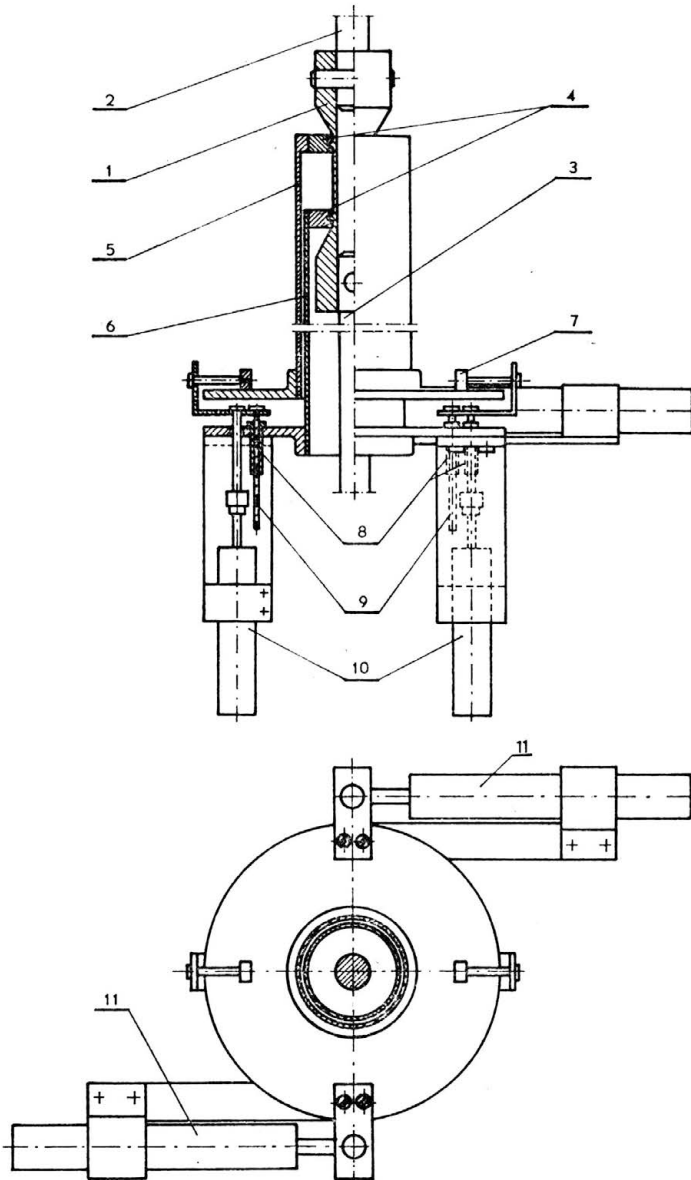


FIG. 6. Extensometer: 1—specimen, 2—upper loading rod, 3—lower loading rod, 4—clamping ring, 5—upper leg of extensometer, 6—lower leg of extensometer, 7—bearing, 8—bush, 9—mandrel, 10, 11—transducers.

nates friction from the torsional loading system. The air is supplied at the pressure of 0.8 MPa from the compressor. The device is also equipped with ball (3—Fig. 5) and roller bearings (4) which serve to prevent the interaction of loading systems when failure of the air supply occurs. The testing creep machine is suitable for tests with cyclic loadings owing to two separate pulley-wire systems transmitting equal and opposite moments of forces.

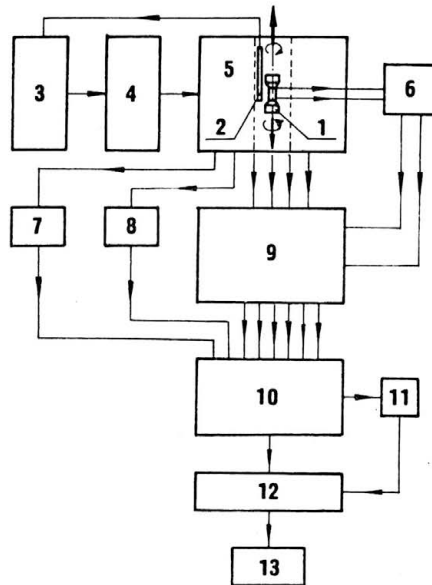


FIG. 7. Diagram of testing stand: 1—specimen, 2—platinum temperature sensor, 3—temperature controller, 4—resistance controller, 5—furnace, 6—thermostat, 7, 8—bridge MT10, 9—bridge TT-6B, 10—clock and switch of channels unit, 11—switch of printer unit, 12—printer control unit, 13—printer.

For investigations at elevated temperatures up to 873 K, a furnace with three heating coil sections was used. Control system used for temperature control allowed for maintaining a constant value of temperature to within the accuracy of  $\pm 1$  K in the whole range of the furnace operation. Temperature at the specimen surface was measured by two thermocouples.

Mechanical extensometer (Fig. 6) and electronical measurement system (Fig. 7) was designed to measure and record the strains of the specimen. The extensometer consisted of two coaxial tubes connected with the specimen by special grips. The extensometer allows for independent measurement of angle of rotation and elongation of the specimen by separating two strain measurement systems; to that end, a system of teflon bearings and guide cores is used. Two transducers for measuring the axial strains and the angle of relative rotation are connected with the lower ends of the tubes traced out of the furnace. Strain measurement is based on recording the linear motion of the cores of the transducers. The induced electric signal, after amplification and conversion to a digital form, is recorded on a paper tape by a printer. The testing device is equipped with a quartz clock for data recording at suitable time intervals.

#### 4. Determination of the surface of constant rate of energy dissipation at steady creep

The programme of tests comprised creep experiments under plane state of stress which were obtained by means of various combinations of tension and torsion at the temperature of 573 K for annealed electrolytic M1E copper. Specimens were maintained at the tempera-



ture of 573 K for 24 hours before the creep test in order to obtain thermal balance at the gauge part of the specimen. Surfaces of constant rate of energy dissipation satisfy the relation

$$(12) \quad L = \sigma_i \cdot D_i = \text{const},$$

where  $\sigma_i = \left(\frac{3}{2} \sigma_{ij} \sigma_{ij}\right)^{1/2}$  —equivalent stress,  $D_i = \left(\frac{2}{3} D_{ij} D_{ij}\right)^{1/2}$  —equivalent strain rate at steady stage of creep.

The surfaces were determined from the creep tests performed according to the programme shown in Fig. 8. Tests were carried out at three values of equivalent stress  $\sigma_i$ ; equal

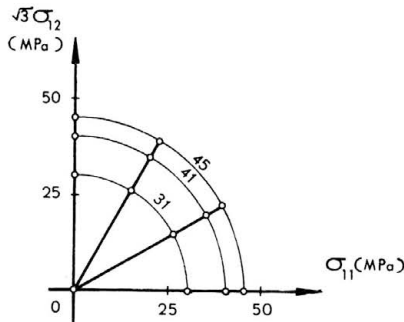


FIG. 8. Programme used for determining the surface of constant rate of energy dissipation under creep.

to 31, 41 and 45 MPa which are lower than the yield point of the considered material at the temperature of 573 K ( $\sigma_{0,2} = 50$  MPa). Thus the total strain is expressed by the relation

$$(13) \quad \varepsilon_{ij} = \varepsilon_{ij}^e + \varepsilon_{ij}^c,$$

where components with a superscript *e* and *c* denote the elastic and creep strains, respectively. For each stress level the tests were performed for points lying in the two-dimensional space of stresses  $(\sigma_{11}, \sqrt{3} \sigma_{12})$ , at the rectilinear trajectories defined by angle  $\theta_\sigma^* = (0^\circ, 30^\circ, 60^\circ, 90^\circ)$ .

The duration of tests, 150 hours, enabled us to determine the steady creep rate.

The creep curves for the stress level of 41 MPa are presented in Fig. 9, while data for the whole experimental programme are summarized in Table 1.

The experimentally obtained steady creep rates can be approximated by using a modified Norton's formula in which the material constants are replaced by functions depending on the direction of loading trajectory. Thus the material parameters must be determined separately for each direction considered.

The values of constants  $\sigma_0, D_0$  are found from the creep results obtained at  $\sigma_i = 31$  MPa.

In order to determine the value of the exponent *n*, diagrams of the dimensionless steady creep rate  $D_i/D_0$  as functions of the dimensionless stress  $(\sigma_i/\sigma_0)$  are drawn in logarithmic

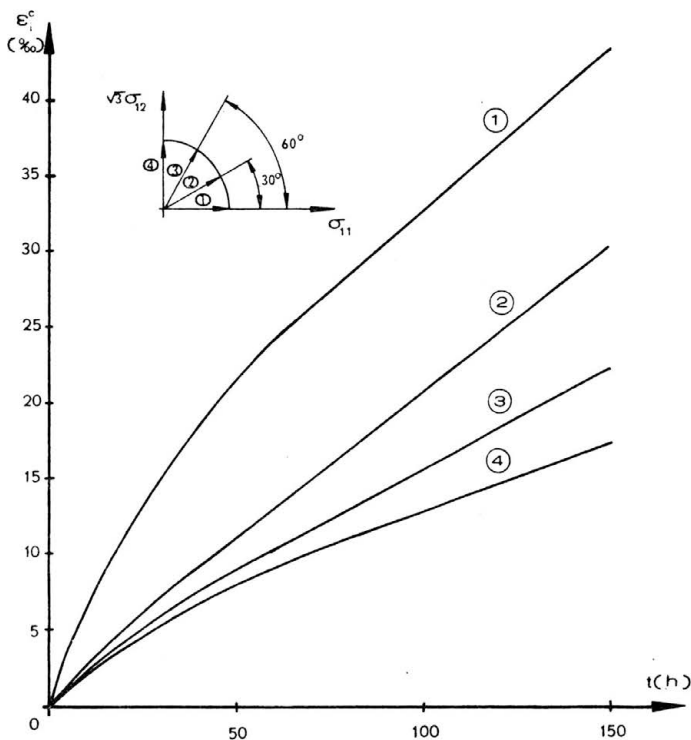


FIG. 9. Creep curves for M1E copper at temperature of 573 K under  $\sigma_1 = 41$  MPa.

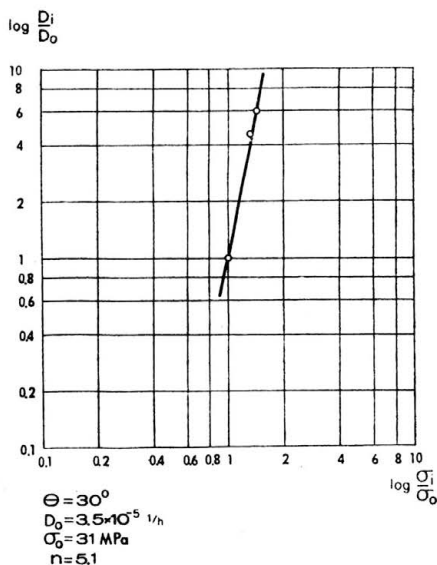
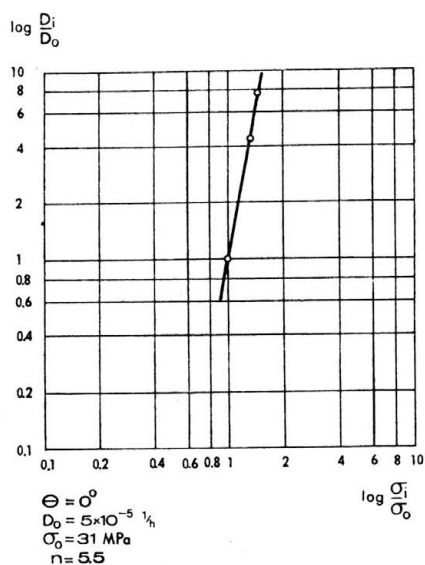


FIG. 10. Diagrams of steady creep rate as a functions of stress in logarithmic scale used for determining value of  $n$ .

Table 1.

$\theta_\sigma$	$\sigma_t = 31$ MPa					$\sigma_t = 41$ MPa					$\sigma_t = 45$ MPa				
	$\sigma_{11}$	$\sigma_{12}$	$D_{11}$	$D_{12}$	$D_t$	$\sigma_{11}$	$\sigma_{12}$	$D_{11}$	$D_{12}$	$D_t$	$\sigma_{11}$	$\sigma_{12}$	$D_{11}$	$D_{12}$	$D_t$
	[MPa]	[MPa]	$\times 10^{-5}$ [1/h]	$\times 10^{-5}$ [1/h]	$\times 10^{-5}$ [1/h]	[MPa]	[MPa]	$\times 10^{-5}$ [1/h]	$\times 10^{-5}$ [1/h]	$\times 10^{-5}$ [1/h]	[MPa]	[MPa]	$\times 10^{-5}$ [1/h]	$\times 10^{-5}$ [1/h]	$\times 10^{-5}$ [1/h]
0	31	—	5	—	5	41	—	22.1	—	22.1	45	13	38	—	38
30	26,8	8.9	3.2	1.2	3.5	35.5	11.8	14.5	6.2	16	39	—	19.2	7.3	21
60	15.5	15.5	1.8	2.2	3.1	20.5	20.5	7.5	9.8	13.5	22.5	22.5	10.5	13.2	18.5
90	—	17.9	—	2	2.3	—	23.7	—	7.8	9	—	26	—	11.3	13

$\sigma_{11}$ —tensile stress,  $\sigma_{12}$ —shear stress,  $D_{11}$ —axial component of steady creep rate,  $D_{12}$ —shear component of steady creep rate,  $D_t$ —equivalent of steady creep rate.

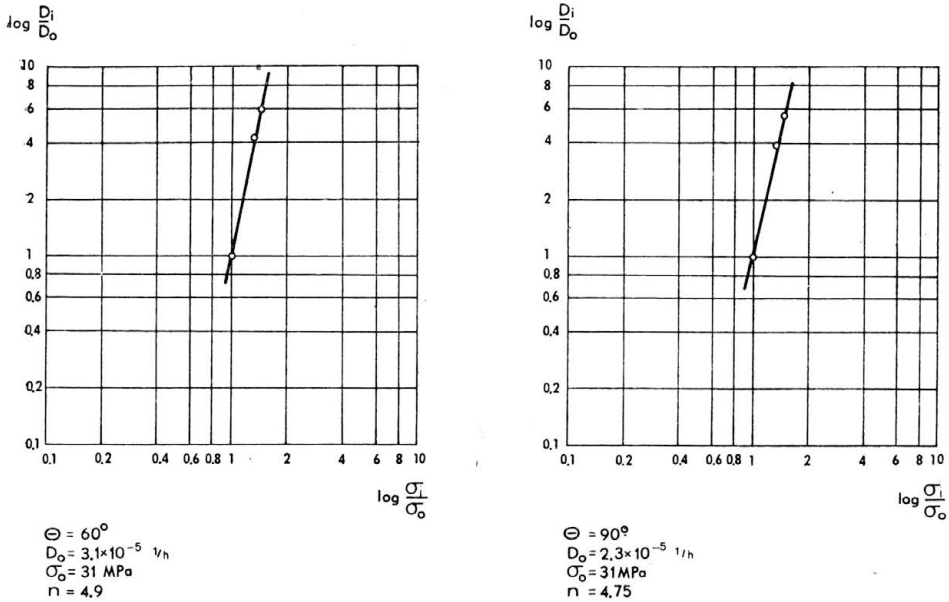


FIG. 11. Diagrams of steady creep state as a function of stress in logarithmic scale used for determining value of  $n$ .

scale (Figs. 10, 11). Experimental points, shown at these diagrams, are distributed along a straight line, tangent of its slope angle being equal to the exponent  $n$ ,

$$(14) \quad \operatorname{tg} \varphi = n = \frac{\log(D_i/D_0)}{\log(\sigma_i/\sigma_0)}.$$

Values of that constant for the direction of the trajectory considered are shown in Figs. 10, 11.

In order to obtain constants for an arbitrary direction of the equivalent stress vector, in the range of  $0^\circ \leq \theta_\sigma \leq 90^\circ$ , experimental values were approximated by a function written in a general form,

$$(15) \quad f(x) = ax^2 + bx + c,$$

and then

$$n(x = \theta_\sigma) = 6.94 \cdot 10^{-5}x^2 - 14.4 \cdot 10^{-3}x + 5.49,$$

$$D_0(x = \theta_\sigma) = 1.94 \cdot 10^{-9}x^2 - 4.58 \cdot 10^{-7}x + 4.925 \cdot 10^{-5}.$$

Graphical representation of values  $n$  and  $D_0$  as functions of the slope angle of the equivalent stress vector is shown in Fig. 12. Solid lines correspond to the approximate function, while points represent the experimental data.

The surfaces of constant rate of energy dissipation were determined on the basis of the function  $n = f(\theta_\sigma)$ ,  $D_0 = f(\theta_\sigma)$  found before and by assuming the equation of the steady creep state in the form  $D_i/D_0 = (\sigma_i/\sigma_0)^n$ . Hence, a given value of the dissipation power which satisfies the condition  $L = \text{const}$  is represented, in the stress space  $(\sigma_{11}, \sqrt{3}\sigma_{12})$ ,

by points of positions defined by the direction  $\theta_\sigma$  and by the length of the equivalent stress vector determined from the relation

$$(16) \quad \sigma_i(\theta_\sigma) = \left[ \frac{L \cdot \sigma_0^n(\theta_\sigma)}{D_0(\theta_\sigma)} \right]^{\frac{1}{n(\theta_\sigma)+1}}$$

Examples of the creep surfaces obtained in the manner described above are presented in Fig. 13 for two values of the dissipation power:  $L = 155 \cdot 10^{-5}$  MPa/h (which corresponds to the dissipation power in the creep test for  $\sigma_i = 31$  MPa and  $\theta_\sigma = 0^\circ$ ) and  $L = 906.1 \cdot 10^{-5}$  MPa/h (which corresponds to the dissipation power in the creep test

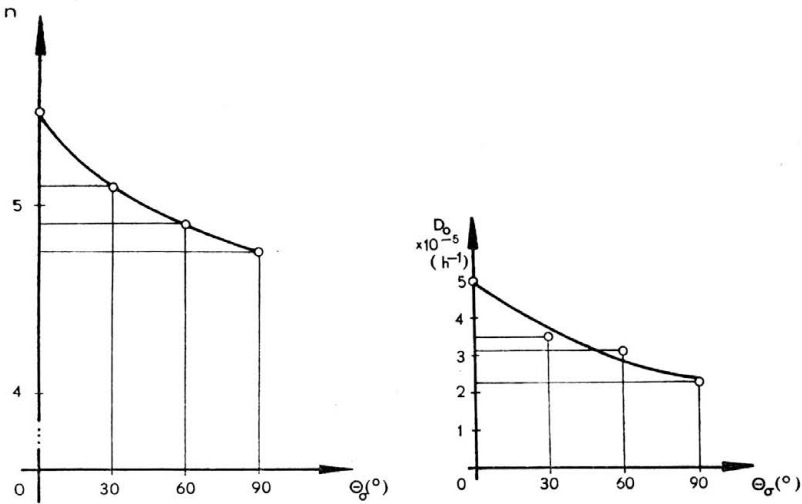


FIG. 12. Values of material constants  $n, D_0$  for M1E copper.

for  $\sigma_i = 41$  MPa and  $\theta_\sigma = 0^\circ$ ). The surfaces calculated according to the potential theory, the creep potential being assumed in form of the second invariant of the stress deviator, are shown by dashed lines.

The experimental results which were used to determine the surfaces of constant rate of energy dissipation show that the annealed material with isotropic mechanical properties in the sense of its yield point and tensile strength under monotonically increasing loading exhibits anisotropy under creep conditions. The maximum difference of creep rates at a steady creep, for a given stress level, lies between the tensile ( $\theta_\sigma = 0^\circ$ ) and torsional ( $\theta_\sigma = 90^\circ$ ) directions for the experimental programme performed. As it is shown in Fig. 13, the anisotropy defined as the ratio of the stress levels for those directions at a given  $L$  exceeds 12%. This is more than twice the value of the rate at tension as compared with that at torsion. Therefore, surfaces of constant rate of energy dissipation can not be determined from the theory assuming the creep potential to be expressed in the same manner as the Huber-Mises condition.

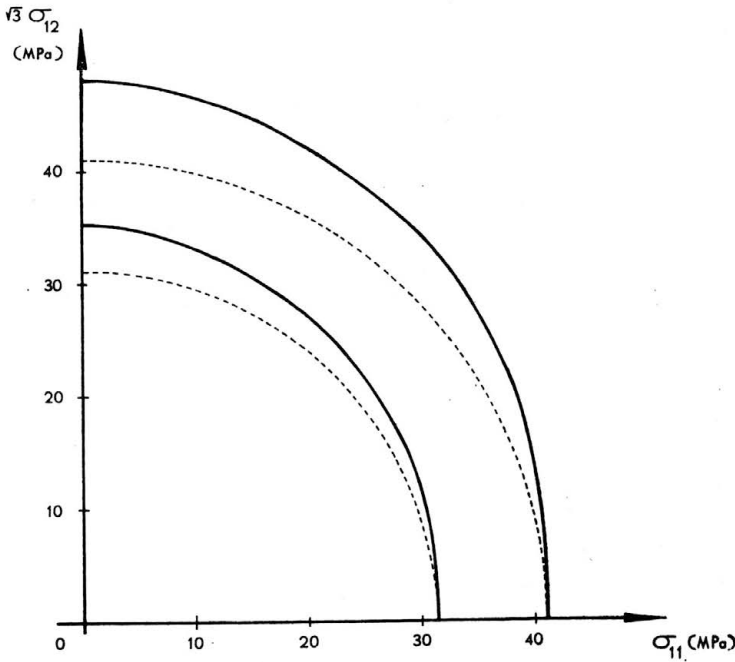


FIG. 13. Surfaces of a constant rate of dissipation energy under steady creep of M1E copper at temperature of 573 K.

## 5. Conclusions

It has been shown that special methods of description of experimental data are necessary to analyze the creep testing under complex state of stress. The concept based on determination of the creep surface is now considered as one of the most effective methods of description of material deformation in time-dependent processes. From the engineering point of view such an approach seems to be most suitable because it yields information on the material behaviour at different states of stresses in a very concise form.

A series of experiments on copper under plane state of stress has been presented in the paper. Results of the tests were used to determine the surfaces of constant rate of energy dissipation.

The material tested possessing isotropic properties at monotonic loading exhibits anisotropy under creep what is manifested by the fact that the creep curves at a given stress level but different paths of proportional loading do not coincide. Therefore the experimental results could not be described by surfaces resulting from the potential theory due to which the creep potential has the form of the second invariant of the stress deviator.

In order to determine the surface of constant power of dissipation, material anisotropy under creep being taken into account, the procedure is proposed based on the assumption that the material constants are actually functions depending on the direction of the equivalent stress vector.

## References

1. J. J. BLASS, W. N. FINDLEY, *Short-time, biaxial creep of an aluminum alloy with abrupt changes of temperature and state of stress*, J. Appl. Mech., **38**, 489, 1971.
2. R. MARK, W. N. FINDLEY, *Concerning a creep surface derived from a multiple integral representation for 304 stainless steel under combined tension and torsion*, J. Appl. Mech., **45**, 773, 1978.
3. C. OYTANA, P. DELOBELLE, A. MERMET, *Constitutive equations study in biaxial stress experiments*, ASME J. Engin. Mat. Tech., **104**, 1, 1982.
4. C. R. CALLADINE, D. C. DRUCKER, *Nesting surface of constant rate of energy dissipation in creep*, Q. Appl. Math., **20**, 79, 1962.
5. W. SZCZEPIŃSKI, *On the effect of plastic deformation on yield condition*, Arch. Appl. Mech., **2**, 15, 1963.
6. W. A. TRĄPCZYŃSKI, *The influence of cold work on the creep of copper under biaxial states of stress*, Acta Metall., **30**, 1035, 1982.
7. Z. MRÓZ, W. A. TRĄPCZYŃSKI, *On the creep hardening rule for metals with memory of maximal prestress*, Int. J. Solids Struct., **20**, 467, 1984.
8. M. WANIEWSKI, *The influence of direction and values of initial plastic deformation on creep of metals*, IFTR Report 34/1983.

POLISH ACADEMY OF SCIENCES  
INSTITUTE OF FUNDAMENTAL TECHNOLOGICAL RESEARCH.

Received December 27, 1985.

---